

Direct Ellipse Fitting and Measuring Based on Shape Boundaries

Milos Stojmenovic and Amiya Nayak

SITE, University of Ottawa,
Ottawa, Ontario, Canada K1N 6N5
{mstoj075, anayak}@site.uottawa.ca

Abstract: Measuring ellipticity is an important area of computer vision systems. Most existing ellipticity measures are area based and cannot be easily applied to point sets such as extracted edges from real world images. We are interested in ellipse fitting and ellipticity measures which rely exclusively on shape boundary points which are practical in computer vision. They should also be calculated very quickly, be invariant to rotation, scaling and translation. Direct ellipse fitting methods are guaranteed to specifically return an ellipse as the fit rather than any conic. We argue that the only existing direct ellipse fit method does not work properly and propose a new simple scheme. It will determine the optimal location of the foci of the fitted ellipse along the orientation line (symmetrically with respect to the shape center) such that it minimizes the variance of sums of distances of points to the foci. We next propose a novel way of measuring the accuracy of ellipse fits against the original point set. The evaluation of fits proceeds by our novel ellipticity measure which transforms the point data into polar representation where the radius is equal to the sum of distances from the point to both foci, and the polar angle is equal to the one the original point makes with the center relative to the x -axis. The linearity of the polar representation will correspond to the quality of the ellipse fit for the original data. We also propose an ellipticity measure based on the average ratio of distances to the ellipse and to its center. The choice of center for each shape impacts the overall ellipticity measure. We discuss two ways of determining the center of the shape. The measures are tested on a set of shapes. The proposed algorithms work well on both open and closed curves.

Keywords: Ellipticity, ellipse fitting, linearity, shape analysis.

1 Introduction

Classifying a shape as a certain primitive is important in image processing applications and computer vision systems. Popular shape measures such as elongation, convexity and orientation exist in literature. Like other measures for primitive geometric shapes, the measure of ellipticity and ellipse fitting are motivated by real world image processing problems. Ellipticity is common in nature and industry, and finding a way of identifying it can be important to both. Applications of

ellipse identification are found in agricultural and medical imaging systems for identifying certain grains, onions, watermelons, cells, and even human faces. In this article we study two related problems: ellipse fitting and measuring shape ellipticity. Finding an ellipse that best represents a set of points is called ellipse fitting. We are also interested in measuring how elliptical a finite set of points is.

The two main approaches to ellipse fitting and measuring ellipticity are shape (boundary) based and area based. Shape based approaches consider only the points on the boundary or perimeter of a shape, while area based ones take into consideration all of the pixels within a closed shape. One of the main advantages of our algorithm is that it works on both open and closed curves. Most other ellipticity measures found in literature are linked to exclusively closed curves, because they are area based. Our algorithms have image processing applications in mind which deal with pixels as points, but also accept real numbers as input. In analyzing various algorithms, we restrict ourselves to the following criteria. Ellipticity values are assigned to sets of points and these values shall be numbers in the range $[0, 1]$. The ellipticity measure equals 1 if and only if the shape is an ellipse, and equals 0 when the shape is highly non-elliptical. A shape's ellipticity value should be invariant under similarity transformations of the shape, such as scaling, rotation and translation. Ellipticity values should also be computed by a simple and fast shape based algorithm. As in existing literature, the points in the set are not ordered; that is, ellipse fits and ellipticity measures do not depend on the ordering of points in the data set or along the boundary. Ellipse fitting has been widely studied in literature. Voss and Süße [16] described an area and moments based method of fitting geometric primitives. Rosin [8, 9] discussed various ellipse fitting methods and various distance measures of points in data sets from the corresponding ellipse fit [11]. We will discuss a shape sampling based method [9] by Rosin because his papers indicate it as the ultimate selection. Fitzgibbon, Pilu and Fisher [4] introduced the only existing direct fitting ellipse method which is heavily based on the work of Bookstein [1]. We will discuss the performance of this method in section 2.

Various ellipticity measures were proposed in literature. An ellipse fit is a prerequisite for some of them. These include DFT and the shape based measure by Proffit [6], the set operations area based method [5], and the Euclidean ellipticity shape based and orthogonal hyperbolae area based measures by Rosin [10]. Other measures are not based on a prior ellipse fit, such as the elliptic variance shape based method [6], and the area and moment based method [10]. Here, we will propose and analyze an algorithm that fits an ellipse to a set of points, and one that finds an ellipticity value for the fitted ellipse. The ellipticity measure can be used to compare quality of several ellipse fits. The ellipse fit is done by first choosing a shape center and finding the orientation line of the shape. The best ellipse fit is chosen by determining the location of the foci of this fit along the orientation line in opposite directions of the shape center. The best locations of the foci are those that minimize the variance of sums of distances of points to the foci. Our new ellipticity measure is based on a measure of linearity used in [14]. Any one of the six linearity measures in [14] can be used as a base of our ellipticity algorithm since the input set of points to our algorithm was transformed from planar representation to polar representation, where highly elliptical input point sets become highly linear in the new representation. This transformation is done by using the center of the shape as the

origin in the polar representation, and by maintaining the angle each point forms with the center. The radius in polar form is modified such that it equals the sum of distances from the point to both foci. The choice of center of each shape influences its overall ellipticity value. The center of each shape is traditionally seen as its center of gravity. We propose to also use a true center (X_{tc}, Y_{tc}) of a shape, defined as the center of a circle C that best fits the shape to C . It is determined by sampling k triplets of points from the point set, and finding their true centers. The median center value of the k samples is taken as the shape's true center. Our algorithms were tested in several ways. The new foci distance variance fit method is compared to the sampling [9] and EllipVos [16] methods using our new polar linearity and average distance ratio measures of ellipticity. The two fit measures from [5, 10], are compared with our two measures on a set of open or closed shapes, as appropriate.

Overall in this paper, we propose two novel algorithms, which when combined fit and assign ellipticity values to sets of planar 2D points. The literature review is given in section 2. The new measures are presented in section 3. Chapter 4 is reserved for the presentation of our test set along with a general discussion of our results.

2 Literature Review

2.1 Central Moments and Orientation of a Point Set

The central moment of order pq of a set of points Q is defined as:

$$\mu_{pq} = \sum_{x,y \in Q} (x - x_c)^p (y - y_c)^q,$$

where S is the number of points in the set Q . The center of gravity (x_c, y_c) is the average value of each coordinate in set Q , and is determined as follows:

$$(x_c, y_c) = \left(\frac{1}{S} \sum x_i, \frac{1}{S} \sum y_i \right),$$

where (x_i, y_i) , $1 \leq i \leq S$, are real coordinates of points from Q . The angle of orientation of the set of points Q is determined by [2]:

$$angle = 0.5 \arctan \left(\frac{2\mu_{11}}{\mu_{20} - \mu_{02}} \right).$$

2.2 Ellipse Fitting by Sampling

Rosin [9] described the least median of squares (LMedS) shape based approach to ellipse fitting. Several (k) minimal subsets (i.e. five points) of the data are selected at random and used to generate the ellipses through them. Only subsets that generate coherent results are considered. When enough minimal subsets have been acquired to satisfy a pre-determined error estimation threshold, the median value of the k subsets of each ellipse coefficient is taken to define the ellipse fit. This method is not guaranteed to return an ellipse.

2.3 Moment Based Ellipse Fitting

Voss and Süße [16] described a moments and area based method of fitting geometric primitives by ellipses. The data is normalized into a unique canonical frame (a circle with specific radius for the case of ellipse fitting), by applying an affine transform. Given input points, they first find the centroid, and translate all points so that the new centroid is at the origin. Then $\mu_{01} = 0$ and $\mu_{10} = 0$ for the translated shape. They then apply an x -sheering transform which maps (x, y) to (x', y') as follows: $x' = x + \beta y$, $y' = y$. The goal is to obtain an elliptical shape with horizontal and vertical axis. For this position, the new moment value of m'_{11} is 0 because such an ellipse is an odd function. This means that

$$\iint_S (x + \beta y) y dx dy = 0, \text{ which decides } \beta = -\mu_{11} / \mu_{02},$$

where μ_{11} and μ_{02} are taken before the transform [12]. The elliptical shape should now be scaled to obtain a circular shape with new unit moments $M_{02} = M_{20} = 1$. The circle with such unit value moments has radius $r = (4/\pi)^{1/4}$ [12]. The new transformation is $x'' = \alpha x'$, $y'' = \delta y'$.

$$1 = M_{20} = \iint_{S''} x''^2 dx'' dy'' = \iint_{S'} (\alpha x')^2 \alpha dx' \delta dy' = \alpha^3 \delta \mu'_{20},$$

and similarly $1 = M_{02} = \alpha \delta^3 \mu'_{02}$. Moments μ'_{02} and μ'_{20} of the shape are calculated after x -shearing and before scaling. Multiplication gives $(\alpha \delta)^4 \mu'_{02} \mu'_{20}$, which leads to $\alpha = (\mu'_{02} / \mu'_{20})^{1/8}$, $\delta = (\mu'_{20} / \mu'_{02})^{1/8}$. This decides the new transform, which brings the data to a circular form with a unique canonical frame.

Applying an inverse transforms to the circle will result in getting the elliptical fit for the original data. A circle with radius r is scaled back to an ellipse with axes $a = r/\alpha$, $b = r/\delta$. The equation of that ellipse is $x'^2/a^2 + y'^2/b^2 = 1$. After inverse x -shearing, the equation of the original ellipse is $(x + \beta y)^2/a^2 + y^2/b^2 = 1$.

2.4 Direct Least Square Fitting

Fitzgibbon, Pilu, Fisher [4] described a direct method for least square fitting of ellipses. The method is based on the method by Bookstein [1] for fitting conic sections to scattered data. The method in [4] is ellipse-specific, so it always returns an ellipse.

The equation $\mathbf{a}'\mathbf{x} = ax^2 + bxy + cy^2 + dx + ey + f = 0$, where $\mathbf{a} = [a \ b \ c \ d \ e \ f]^T$ and $\mathbf{x} = [x^2 \ xy \ y^2 \ x \ y \ 1]^T$ describes an arbitrary conic section \mathbf{a} . This conic section is an ellipse if $b^2 - 4ac < 0$.

Given a point (x_i, y_i) , its algebraic distance to conic \mathbf{a} from a point to a candidate ellipse is $\mathbf{a}'\mathbf{x}_i$ where $\mathbf{x}_i = [x_i^2 \ x_i y_i \ y_i^2 \ x_i \ y_i \ 1]^T$. The method [1] minimizes the sum of squared algebraic distances $G = \sum_{i=1}^N (\mathbf{a}'\mathbf{x}_i)^2$, where \mathbf{x}_i are the input points.

Let $\mathbf{D} = [\mathbf{x}_1 \ \mathbf{x}_2 \ \dots \ \mathbf{x}_N]^T$, and $\mathbf{S} = \mathbf{D}^T \mathbf{D}$ (called the scatter matrix, a symmetric 6x6 matrix). Then $G = (\mathbf{D}\mathbf{a})^T (\mathbf{D}\mathbf{a}) = \mathbf{a}^T \mathbf{D}^T \mathbf{D} \mathbf{a} = \mathbf{a}^T \mathbf{S} \mathbf{a}$. Therefore the problem is to minimize $G = \mathbf{a}^T \mathbf{S} \mathbf{a}$. However, a constraint on coefficients needs to be placed, since otherwise

the solution is not unique. Bookstein [1] suggested to use constraint $a^2 + b^2/2 + c^2 = 2$. We follow here the description and solution of [1] since [4] only discussed the difference from that algorithm. This solution is generally applicable for any constraint of the form $\mathbf{a}^T \mathbf{C} \mathbf{a} = \text{constant}$. The main contribution of [4] is to replace the diagonal constraint matrix \mathbf{C} by a matrix which corresponds to the condition $4ac - b^2 = 1$, which then always produces an ellipse. Such a matrix \mathbf{C} satisfies $\mathbf{a}^T \mathbf{C} \mathbf{a} = 1$ and has all zeros except $C_{13} = C_{31} = 2$, $C_{22} = -1$. Let $\mathbf{a}^T = (\mathbf{a}_1^T \mid \mathbf{a}_2^T) = [a \ b \ c \mid d \ e \ f]$. Let \mathbf{S} be decomposed into four blocks, where \mathbf{S}_{11} , $\mathbf{S}_{12} = \mathbf{S}_{21}^T$ and \mathbf{S}_{22} are 3x3 matrices. Then $G = \mathbf{a}^T \mathbf{S} \mathbf{a} = \mathbf{a}_1^T \mathbf{S}_{11} \mathbf{a}_1 + 2\mathbf{a}_1^T \mathbf{S}_{12} \mathbf{a}_2 + \mathbf{a}_2^T \mathbf{S}_{22} \mathbf{a}_2$. The constraint is on \mathbf{a}_1 , not on \mathbf{a}_2 . Assuming \mathbf{a}_1 is fixed, the minimum for G is obtained when $d(\mathbf{a}^T \mathbf{S} \mathbf{a}) / (d\mathbf{a}_2) = 0$. Using theorems of matrix calculus, this means that $2\mathbf{a}_1^T \mathbf{S}_{12} + 2\mathbf{a}_2^T \mathbf{S}_{22} = 0$, or $\mathbf{a}_2^T = -\mathbf{a}_1^T \mathbf{S}_{12} \mathbf{S}_{22}^{-1}$. Then $G = \mathbf{a}_1^T \mathbf{S}_{11} \mathbf{a}_1 + \mathbf{a}_1^T \mathbf{S}_{12} \mathbf{a}_2 = \mathbf{a}_1^T (\mathbf{S}_{11} - \mathbf{S}_{12} \mathbf{S}_{22}^{-1} \mathbf{S}_{21}) \mathbf{a}_1 = \mathbf{a}_1^T \mathbf{S}_1 \mathbf{a}_1$, $\mathbf{S}_1 = \mathbf{S}_{11} - \mathbf{S}_{12} \mathbf{S}_{22}^{-1} \mathbf{S}_{21}$. The problem now is to minimize $\mathbf{a}_1^T \mathbf{S}_1 \mathbf{a}_1$ subject to $\mathbf{a}_1^T \mathbf{C}' \mathbf{a}_1 = 1$, where \mathbf{C}' is the top 3x3 sub-matrix from \mathbf{C} (nonzero elements are $C'_{13} = C'_{31} = 2$, $C'_{22} = -1$).

The Lagrange multiplier λ is introduced, to minimize $\mathbf{a}_1^T \mathbf{S}_1 \mathbf{a}_1 - \lambda \mathbf{a}_1^T \mathbf{C}' \mathbf{a}_1$. The derivative with respect to \mathbf{a}_1^T implies $2\mathbf{S}_1 \mathbf{a}_1 - 2\lambda \mathbf{C}' \mathbf{a}_1 = 0$. λ is a relative eigenvalue of \mathbf{S}_1 with respect to \mathbf{C}' , or a solution to $|\mathbf{S}_1 - \lambda \mathbf{C}'| = 0$, and \mathbf{a}_1 is the corresponding eigenvector. The determinant $|\mathbf{S}_1 - \lambda \mathbf{C}'| = 0$ is a cubic polynomial in λ . The eigenvectors for each real solution λ are obtained from $(\mathbf{S}_1 - \lambda \mathbf{C}') \mathbf{a}_1 = 0$. Usually the best solution corresponds to the smallest λ [1]. Let $\mathbf{H} = \mathbf{S}_1 - \lambda \mathbf{C}'$ and $\mathbf{u} = (a \ b \ c)^T$ be a solution of this homogeneous 3x3 system $\mathbf{H} \mathbf{u} = 0$ (one can fix $c = 1$). Then $\mu \mathbf{u}$ is also a solution for any μ , and $\mathbf{a}_1 = \mu \mathbf{u}$ satisfies constraint $\mathbf{a}_1^T \mathbf{C}' \mathbf{a}_1 = 1$. Thus $\mu^2 \mathbf{u}^T \mathbf{C}' \mathbf{u} = 1$ and $\mu = (1 / (\mathbf{u}^T \mathbf{C}' \mathbf{u}))^{1/2}$. The conic we looked for is $\mu \mathbf{u} = (a \ b \ c)^T$ while $\mathbf{a}_2^T = (d \ e \ f)$ is obtained from $\mathbf{a}_2^T = -(\mu \mathbf{u})^T \mathbf{S}_{12} \mathbf{S}_{22}^{-1}$.

It can be observed, however, that scaling input data \mathbf{D} leads to the scaling of the matrices \mathbf{S} and \mathbf{S}_1 without changing constraint \mathbf{C}' and therefore changes the cubic polynomial $|\mathbf{S}_1 - \lambda \mathbf{C}'| = 0$. This will change the claimed optimal values for λ and \mathbf{a}_1 , as confirmed by our implementation, without ever producing a visually good fit. We believe that the optimal fit should be scalable and therefore conclude that the method [1, 4] does not work.

2.5 DFT Based Ellipticity Measure

Proffitt [6] described a shape based approach for measuring ellipticity based on the discrete Fourier transform (DFT). An ellipse is fitted to the shape by centering it on the shape's centroid. The ellipse is then scaled such that its mean square of the lengths of the lines from the centroid to the boundary points matches the shape's. Let $u[j] = a[j] + ib[j]$, $i = \sqrt{-1}$, and $v[j] = x[j] + iy[j]$ be the corresponding points on the ellipse and the shape boundary, with the line between them passing through the centroid. Then the ellipticity measure D [6] (not normalized to [0, 1]) is $D^2 = \frac{1}{2N} \sum_{j=1}^N (u[j] - v[j])^2$. Note that $(u[j] - v[j])^2 = (a[j] - x[j])^2 + (b[j] - y[j])^2$ is the Euclidean distance.

2.6 Area Comparison to Measure Ellipse Fit

Koprnicky, Ahmed, and Kamel [5] defined ellipticity measures based on comparing the areas of shape S , the area of its ellipse fit R , and the areas of set differences SVR

and RS between the two. The measure that is closest to our criteria is $(\text{area}(SR) + \text{area}(RS)) / (\text{area}(S \cup R))$. The authors do not elaborate on how to determine the best ellipse fit. This measure however might produce results that are outside of the interval $[0, 1]$ when the ellipse fit is much bigger than the shape it is trying to fit. We therefore modified their method to measure ellipticity via $\text{area}(S \cap R) / \text{area}(S \cup R)$.

2.7 Moment Based Ellipticity Measures

An area based ellipticity measure of a fit is obtained by comparing the differences between the central moments u_{ij} and u'_{ij} of the shape and the corresponding ellipse fit [10, 13]. The measure is

$$\frac{1}{1 + \sum_{i,j=0}^{i+j \leq 4} (\mu'_{ij} - \mu_{ij})^2}.$$

This method relies on normalizing u_{ij} coefficients, normally gives number close to 0, and can be used to rank shapes. Rosin [10] defined another moment based ellipticity measure as follows. Since any ellipse can be obtained by applying an affine transform to a circle, the simplest affine moment invariant of the circle can be used to characterize ellipses. It is defined as $I = (\mu_{20}\mu_{02} - \mu_{11}^2) / \mu_{00}^4$, where μ_{pq} are central moments. The moment for the unit radius circle is $I_c = 1/(16\pi^2)$. Thus I is measured for a given shape, and the measure of ellipticity of that shape in [10] is: $E = 16\pi^2 I$ if $I \leq 1/(16\pi^2)$, or $1/(16\pi^2 I)$ otherwise.

2.8 Elliptic Variance Based Ellipticity Measure

Peura and Iivarinen [7] described an ‘elliptic variance’ which they used to measure ellipticity based on shape perimeters. The center of gravity $\mathbf{u} = (u_1, u_2)^T$ and the covariance C of N data points $\mathbf{p}_i = (x_i, y_i)^T$ are calculated. Covariance is a 2x2 matrix and is calculated by the following formula:

$$C = \frac{1}{N} \sum_{j=1}^N (\mathbf{p}_i - \mathbf{u})(\mathbf{p}_i - \mathbf{u})^T.$$

The mean radius v of the contour is $v = \frac{1}{N} \sum_{i=1}^N \sqrt{(\mathbf{p}_i - \mathbf{u})^T C^{-1} (\mathbf{p}_i - \mathbf{u})}$.

The elliptic variance is then $EVAR = \frac{1}{Nv^2} \sum_{i=1}^N \left(\sqrt{(\mathbf{p}_i - \mathbf{u})^T C^{-1} (\mathbf{p}_i - \mathbf{u})} - v \right)^2$.

Rosin [10] modified it to get a measure in $[0, 1]$ as follows: $PI = 1/(1+EVAR)$. He observed that $EVAR$ suffers from the same problems as many distance approximations used for ellipse fitting. In particular, similar to standard algebraic distance, it exhibits a curvature bias (distances near the pointed ends of the ellipse are underestimated relative to distances at the flatter sections). This leads to irregularities at the ends having less of an effect than at the sides. However, it is not prone to the asymmetry between distances inside and outside the fitted ellipse.

2.9 Orthogonal Hyperbolae Distance and Ellipticity Measure

Rosin described a number of metrics for calculating the approximate error of each point, which represents the distance the point deviates from the fit [8, 11]. The true point error – the distance from the point along the line normal to the ellipse, involves solving a quartic equation. Rosin recommended [10] using the method that approximates the normal distance to an ellipse by the distance to the intersection with the confocal orthogonal hyperbolae passing through the point [8]. The ellipse fit error is then robustly and accurately determined by the summed errors of the ellipse fit as $SE = \sum_{i=1}^N d_i$, where d_i are the orthogonal hyperbolae based distance approximations [8] and N is the number of points to fit. Rosin [10] then proposed the following area based ellipticity measure: $EE = (1 + SE / (N \sqrt{A}))^{-1}$ (A is the area of given shape).

2.10 Detecting Elliptical Shapes

[15] described a variety of shape measures, applying them as shape descriptors of saccular otoliths. They list a number of shape measures from literature for measuring aspect ratio (elongation), compactness, convexity, eccentricity, rectangularity, ellipticity, circularity [6], triangularity [16], convexity, intrusiveness, protrusiveness, and several further measures. [3, 17] consider the problem of detecting ellipses, but do not measure ellipticity in the process. David [3] studied the problem of detecting cereal grains considering them as ellipses with aspect ratios (elongation) close to 2:1. They detect ellipses based on the property that the line passing through the centers of two horizontal chords also passes through the center of ellipse. A Hough transform was applied to handle some irregularities when grains touch each other.

Zhang and Liu [17] described an ellipse detector that may be used for real-time face detection. They first extract edges from the image using a robust edge detector. The center of an ellipse is detected by intersecting two lines that pass through the intersection of tangent lines and the midpoint of the corresponding chord. The parameter space of the Hough transform is decomposed to achieve computational efficiency.

2.11 Measuring Linearity

Stojmenovic, Nayak and Zunic [14] proposed 6 linearity measurements for finite, planar point sets. Their measures are quickly calculated and are invariant to scale, translation or rotation. All of their methods give linearity estimates in the range [0, 1] after some normalization. Their *Average Orientations* measure takes k random pairs of points along the curve. It finds their slopes (m), and finds the normals to their slopes ($-m, 1$). These normals are averaged out, and the resulting normal (A, B) is deemed to be the normal to the orientation of the curve. The averaging is done separately for each vector coordinate. The measure of linearity is defined as $\sqrt{A^2 + B^2}$. The *Eccentricity* measure is determined by first finding the center of gravity of the set of points (X_c, Y_c). All of the points are translated by $(-X_c, -Y_c)$ so that the center of gravity is (0, 0). The linearity is determined to be

$$\text{linearity} = \frac{\sqrt{(\mu_{20} - \mu_{02})^2 + 4\mu_{11}^2}}{\mu_{20} + \mu_{02}},$$

where μ_{11} , μ_{02} , and μ_{20} are the second order moments of the shape. The *triangle heights* linearity measure is found by first taking k triplets of random points from the set and computing the heights h to the longest side of the triangles that the triplets form. This h value is divided by the longest side c of the triangle to normalize the measure. This value is called hc . We use the average of these k hc values as a linearity measure of the set of points. The *triangle perimeters* method is similar to the previous one in the sense that k triplets of random points from the set of points are taken. Each triplet of points defines the vertices of a triangle. The three sides of the triangle are labelled a , b and c , where $a \leq b \leq c$. The linearity measure derived from these three sides is $p = (2c - a - b)/c$. The *contour smoothness* measure was formed by taking triplets of points, and averaging out their triangular areas. Each triplet of points produced a *smoothness* value in the form of $\text{area}/\text{perimeter}^2$. The maximum value for area divided by the triangle perimeter is $\sqrt{3}/36$ (for an equilateral triangle). After *smoothness* values are averaged to produce value sums , the result is adjusted as follows: $\text{sums} = 36 \text{sums} / \sqrt{3}$. The compliment of the obtained sums value was taken as a linearity value. The *Ellipse Axis Ratio* was determined by first finding the center of mass and the first and second order moments of the set of input points, and then finding the values of the major and minor axis of the best fit ellipse as determined by the formulas in [9]. The linearity value was given as $1 - \text{minor axis}/\text{major axis}$.

3 Measuring Ellipticity

Our new ellipse measures are presented here in two sections. The first deals with fitting an ellipse to point data, and the second measures the ellipticity of the point set by rating the accuracy of the ellipse fit. The quality of the fit relies on an accurate method of finding the center of the shape. We propose two ways of finding shape center. The standard way is by considering the center of gravity, and the other is by finding the true center of the shape.

3.1 Fitting an Ellipse to a Set of Points

Here we describe the algorithm that fits an ellipse to a set of points. Its input is just the set of points, and it outputs the locations of the optimal foci locations, along with the major and minor axes of the fit ellipse and the angle of orientation of the major axis of the fit ellipse. We begin by finding the angle of orientation α of the point set via moments. The moment based algorithm sometimes produces orientation angles that are normal to the actual shape orientation. To verify the correctness of the obtained value α , the linearity of the set was measured twice. The first measure was made considering the orientation angle was α , and the second was made considering orientation angle $\alpha + 90^\circ$. Linearity can be measured using any one of the linearity measures from [14]. The higher of the two linearity values corresponds to the actual

orientation of the shape. The orientation line passes through the selected center and has slope α . We then project all points onto the orientation line, resulting in a new array. The two extremity points min and max along the orientation line of the new array are found. In Figure 1 we see the blue orientation line which is also the line on which the points on the shape are projected. G is the center of the shape. Foci f_1 and f_2 will be determined by the foci finding procedure to follow.

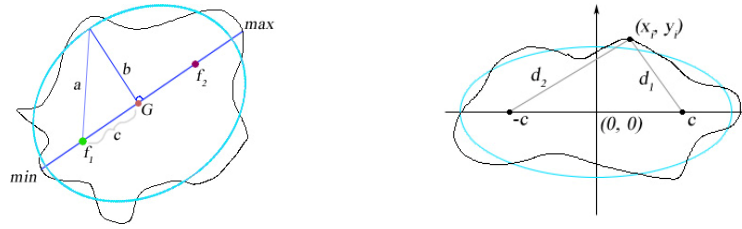


Fig. 1. Orientation line with foci, min , max , a , b , c , and G **Fig. 2.** Variance of summed foci dist.

3.1.1 Finding Optimal Foci for Ellipse Fitting

For simplicity, we assume that the point set has been translated such that its center is at the origin. Also, the point set has been rotated such that its orientation line lies on the x axis.

In Figure 2, the distances to the foci are:

$$d_1 = \sqrt{(x_i - c)^2 + y_i^2}, \text{ and } d_2 = \sqrt{(x_i + c)^2 + y_i^2}.$$

Therefore, we have

$$D_i = d_1 + d_2 = \sqrt{(x_i - c)^2 + y_i^2} + \sqrt{(x_i + c)^2 + y_i^2}.$$

We need to find c for which the values D_i have the smallest possible variance. Variance is defined by:

$$f(c) = (N - 1)\sigma^2 = \sum_{i=1}^N D_i^2 - \frac{1}{N} \left(\sum_{i=1}^N D_i \right)^2.$$

This is a continuous function and thus has a minimum value c such that $f'(c) = 0$.

$$\begin{aligned} f(c) &= \sum_{i=1}^N \left(\sqrt{(x_i - c)^2 + y_i^2} + \sqrt{(x_i + c)^2 + y_i^2} \right)^2 - \frac{1}{N} \left(\sum_{i=1}^N \left(\sqrt{(x_i - c)^2 + y_i^2} + \sqrt{(x_i + c)^2 + y_i^2} \right) \right)^2 \\ \Rightarrow f'(c) &= 2 \sum_{i=1}^N \left(\sqrt{(x_i - c)^2 + y_i^2} + \sqrt{(x_i + c)^2 + y_i^2} \right) \cdot \left(\frac{-(x_i - c)}{\sqrt{(x_i - c)^2 + y_i^2}} + \frac{(x_i + c)}{\sqrt{(x_i + c)^2 + y_i^2}} \right) - \\ &\frac{2}{N} \left(\sum_{i=1}^N \left(\sqrt{(x_i - c)^2 + y_i^2} + \sqrt{(x_i + c)^2 + y_i^2} \right) \right) \cdot \sum_{i=1}^N \left(\frac{-(x_i - c)}{\sqrt{(x_i - c)^2 + y_i^2}} + \frac{(x_i + c)}{\sqrt{(x_i + c)^2 + y_i^2}} \right). \end{aligned}$$

This is a continuous function of one variable, which can be solved by a standard equation root finding technique of numerical analysis, such as the bisection method. Note that, $f(c)$ may have local minima and thus multiple solutions for equation $f'(c)$, some of which could even correspond to local maxima. Therefore solving the problem in this direction is not straight forward. We therefore opted for a simple approximate solution that corresponds to a linear search with pixel unit distance steps.

Foci in our implementation are found by inspecting each possible location for the pair between min and G for f_1 , and G and max for f_2 simultaneously so that $|Gf_1|=|Gf_2|$. For each candidate location foci pair, the distances from each point on the shape to both foci are stored in an array. The variance of this array is calculated for each candidate pair, and the one with the lowest variance corresponds to the best choice for the locations of the ellipse fit foci. Now that foci are found, we need the median of the sum of distances from each point on the shape to both foci in order to find the length of the major axis a , which equals half of this sum. The distance c from focus f_1 to center G is used to find the length of the minor axis $b = \sqrt{a^2 - c^2}$. We now have all of the necessary components of the ellipse fit to be able to evaluate it.

3.2 Assessing the Fit Quality: Minimal Variance of Summed Foci Distances

Once the foci of the ellipse fit have been determined, the quality of the ellipse fit can be assessed. This was done by first transforming the original point set into polar representation. This transformation is seen in Figure 3.

In Figure 3, we see the inherent ellipse property that each point on the ellipse is equidistant to the sum of distances from both foci. We exploit this property when transforming the point set to polar coordinate form. As seen in the bottom part of Figure 3, the polar distance value for each point x from the center G will be the sum of distances from x to both foci, $r = d_1 + d_2$. The angle α that vector Gx' forms with the x -axis will remain the same as the angle Gx formed with the x -axis. For a perfect ellipse, the resulting shape can be drawn as a circle, but if its polar coordinate shapes are plotted as Cartesian, they would look highly linear, as seen in Figure 4.

Applying a linearity measure to this polar representation results in a linearity value for the modified set of points. This linearity value represents the ellipticity value of the original set.

A normalization was applied to the polar coordinate transformation of points since the angles the points form in the new representation is limited to the interval $[0, 360]$, whereas the length of the radii they form is unbounded. This can result in polar representations that are not proportional to the original shape. To normalize the polar representation, the following information is gathered from it: the length of the smallest and largest radii r_{min} , r_{max} , and the variance of the radii, r_{var} . The normalization factor $norm = (360 * r_{var}) / N$.

This normalization factor represents the size of the interval each radius would be fit into. The larger the variance of the radii, the less the points fit to the ellipse. Therefore the interval they are placed in is larger to make the linearity value of this set smaller. Each radius value is normalized by the following statement: $R = norm * (r - r_{min}) / (r_{max} - r_{min})$. The result is a number that fits a radius R into the interval $[0, norm]$.

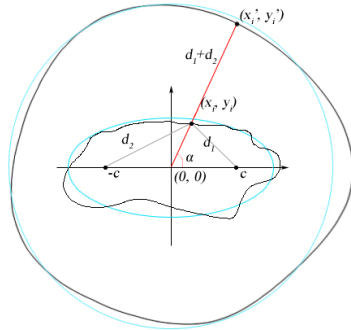


Fig. 3. Transforming the input set to polar representation

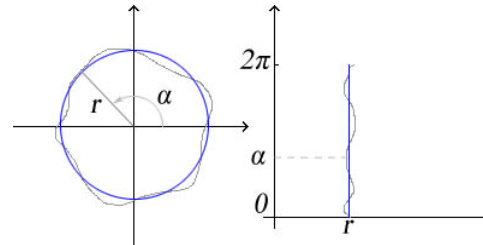


Fig. 4. Polar point set on a planar graph

3.3 Average Distance Ratio to Ellipse and the Center

We propose a shape based ellipticity measure that can be applied to open and closed shapes. Let O be the center of fitted ellipse, and V be a point from the original set. Let U be the intersection of line VO with the fitted ellipse that is closer to V , therefore $|VU| < |VO|$. This intersection can be found by using the equations of a line and ellipse, which leads to a quadratic equation. The error measure used is the average of the distance ration to the ellipse and to the center, that is, $|VU|/|VO|$. It always returns a number between 0 and 1.

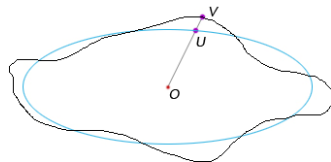


Fig. 5. Finding intersect U on line VO

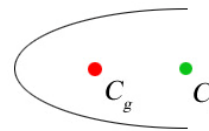


Fig. 6. Choosing the correct shape center

3.4 Finding the Center of a Shape

The trivial way of choosing a shape's center is to take the per-coordinate average of all pixels, which is the center of gravity. This is the method that is usually chosen when measuring any shape property such as linearity, orientability or elongation. Choosing the appropriate center of a shape when measuring ellipticity is more delicate and heavily influences the result of the ellipticity measure.

To illustrate this point, we turn to figure 6. Here, we see a semi elliptical shape where the red dot represents the center of the shape as determined by the traditional method. Transferring the shape to polar coordinates with respect to the red dot would not yield a straight line, but rather a curved one. This would result in a much lower ellipticity measure than expected for the given shape. However, had the green dot been chosen as the center, the resulting polar coordinate representation would have looked similar to the line seen in Figure 4, and a much higher ellipticity measure

would have been awarded. We have experimented with both types of center finding methods in this work. In order to find the ‘true center’ of a shape, as opposed to its traditional center of gravity, we sampled k quintuplets of points from its point set. From each quintuplet, we found the center (X_{tc}, Y_{tc}) that the points define via the method proposed in [9].

4 Experimental Data

The ellipticity algorithms were tested on a set of 20 closed shapes, shown in Figure 7, and 15 open shapes shown in Figure 8. These shapes were assembled by hand and are meant to cover a wide variety of non trivial curves. Each of them is comprised of between 100 and 500 points. This number of pixels is common in extracted edges of some computer vision systems.

The center of gravity was close to the true center in almost all of the closed test curves seen in Figure 7. There are however big differences in the ellipticity values of the shapes seen in Figure 7 because the two centers were generally not close.

Table 1 holds the ellipticity values for closed curves. The three algorithms for ellipse fitting found in table 1 are the new foci variance fitting measure proposed here, the fitting measure proposed by Voss and Sube [16], and Rosin’s sampling LMedS technique [9]. This set of three ellipse fitting techniques was evaluated by two separate ellipticity measures: the ellipticity via linearity measure proposed here (average orientation linearity measure [14] was applied in polar space), and the area based measure proposed by Koprnicky, Ahmed, Kamel (KAK) [5]. The right most column in table 1 shows the ellipticity values of the E measure in [10], which does not rely on an ellipse fit of a shape.

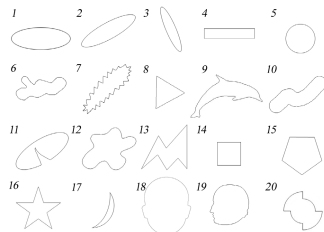


Fig. 7. Closed test curves

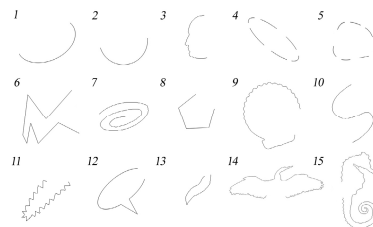


Fig. 8. Open Test Curves

The VS [16] fit algorithm is area based, so to be able to compare it to the shape based ones, the fit it produced based on the area pixels of a shape was evaluated for ellipticity against the perimeter pixels of the same shape. The perimeter pixels were extracted using a 3x3 mask that checked to see if a pixel had at least one neighbour which is not included in the shape. If it had at least one, it was considered as part of the perimeter. Most of the algorithms agree upon the ellipticity results of the figures which are highly elliptic to the naked eye, as seen in table 1. Shape 8 in figure 7 is the first major disagreement between the ellipticity fits and measures. The left two shapes of Figure 7 show the ellipse fit of our algorithm, and the general fit of the rest of the

algorithms for this triangular shape. Our fit is more elongated, and closely follows the triangle on the left hand side. The ellipticity values for this shape vary considerably between measures. Our measure produces the lowest ellipticity value for this shape and we feel that such a low score is merited given that a triangle should not be closely associated with an ellipse.

Table 1. Ellipticity results for closed curves

	Ellipticity Via linearity			KAK			E [10]
	<i>Foci var gc</i>	[16] <i>VS fit</i>	[9] <i>LMedS</i>	<i>Foci var gc</i>	[16] <i>VS fit</i>	[9] <i>LMedS</i>	
1	1	0.98	1	0.95	0.99	0.96	1
2	1	0.97	1	0.94	0.99	0.94	1
3	1	0.98	1	0.96	0.99	0.97	1
4	0.92	0.83	1	0.82	0.92	0.68	0.91
5	1	0.98	1	0.98	1	0.98	1
6	0.83	0.73	0.75	0.68	0.9	0.64	0.72
7	0.99	0.84	0.97	0.8	0.94	0.93	0.9
8	0.27	0.68	0.83	0.59	0.88	0.31	0.68
9	0.51	0.54	0.49	0.44	0.87	0.73	0.35
10	0.84	0.77	0.92	0.77	0.91	0.86	0.76
11	0.99	0.89	0.99	0.84	0.96	0.97	0.87
12	0.75	0.73	0.79	0.69	0.89	0.93	0.78
13	0.77	0.63	0.69	0.24	0.87	0.64	0.55
14	0.4	0.63	0.14	0.34	0.93	0.99	0.91
15	0.85	0.77	0.82	0.89	0.95	0.15	0.97
16	0.45	0.6	NA	0.49	0.86	NA	0.54
17	0.89	0.37	NA	0.45	0.87	NA	0.38
18	0.99	0.45	0.99	0.95	0.44	0.94	0.99
19	0.89	0.32	0.85	0.92	0.33	0.93	0.98
20	0.91	0.39	0.74	0.55	0.94	0.95	0.92

Shape 16 in Figure 7 shares a similar discrepancy in awarded ellipticity scores. The star shape has similar disagreements in ellipticity scores to the triangular shape, and the explanation for these disagreements is also similar. The difference in fits can be seen in the right part of Figure 9. The rest of the closed shapes have ellipse fits and values that very closely follow the original shapes.

Table 2. Ellipticity results for open curves

	Ellipticity Via polar linearity			Distance ratio to ellipse and center		
	<i>Foci var tc</i>	<i>Foci var cg</i>	[9] <i>LMedS</i>	<i>Foci var tc</i>	<i>Foci var cg</i>	[9] <i>LMedS</i>
1	0.94	0.54	0.88	0.97	0.83	0.86
2	0.98	0.66	0.93	0.98	0.82	0.96
3	0.61	0.39	0.40	0.90	0.82	0.88
4	1.00	1.00	1.00	0.97	0.97	0.98
5	0.96	0.98	0.99	0.72	0.75	0.66
6	0.10	0.71	NA	0.74	0.69	NA
7	0.82	0.83	0.80	0.74	0.76	0.66
8	0.82	0.56	0.71	0.92	0.89	0.79
9	0.91	0.62	0.91	0.95	0.92	0.96
10	0.96	0.22	0.97	0.89	0.79	0.78
11	0.93	0.92	0.96	0.92	0.82	0.88
12	0.79	0.92	0.87	0.86	0.83	0.87
13	0.96	0.98	1.00	0.84	0.86	0.66
14	0.92	0.93	0.87	0.77	0.83	0.78
15	0.61	0.69	0.95	0.71	0.72	0.56

Table 2 shows the results of the ellipticity measures as applied to the open curves in Figure 8. Our ellipse fits with true and gravity centers based on minimizing variance of summed distances to foci is compared with sampling LMedS method [9]. Fit accuracies are measured by our two newly proposed methods, polar linearity and average distance ratio to the fitted ellipse and its center.

The choice of center significantly impacts the fit and ellipticity values of the shapes tested here. Shapes 1 and 2 in Figure 7 best illustrate the impact of center selection. In Figure 10, we see these two shapes coupled with their ellipse fits with both the center of gravity and true center approaches. The light blue dots represent the chosen centers for each shape. The ellipticity values for the shapes in Figure 9 are 0.54, 0.94, 0.66, and 0.98 respectively.

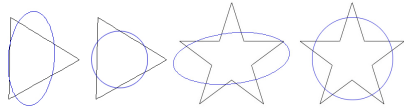


Fig. 9. Ellipticity of a triangle and a star

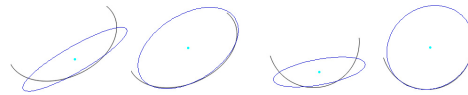


Fig. 10. Center of gravity vs. true center impact

5 Conclusion

Finding the true center of an ellipse greatly improved the fit for open curves. However, the orientation line also heavily influences the overall quality of the fit. If the orientation line is found not to overlap with the actual visual orientation of the shape, the foci finding procedures are forced to find foci locations that are along this erroneous orientation line. This diminishes the ellipticity values for highly elliptical shapes. The LMedS sampling method [9] for finding the true center of a shape does not always return a center since some shapes cannot be easily fit with an ellipse. This is especially true considering the 5 point sampling technique which might not produce quintuplets of points that can be inscribed with just one ellipse. The other problem with the sampling technique is that it might not return an ellipse, but instead either hyperbola or parabola. We have made an extensive literature review, investigation, and implementation of existing methods. Most ellipticity methods from literature do not fit our criteria for a variety of reasons. Most of the methods are area based [5, 16, 4], and some of the ones that are shape based do not return ellipticity values that reflect how elliptical a shape is, rather they can just be used to rank shapes (moment based [10], [6, 7]). Other than LMedS [9] for fitting, our methods appear to be the only ones that are boundary based, guaranteed to return an ellipse, work with open and closed curves, and return meaningful number in the interval [0,1].

References

1. Bookstein, F.L.: Fitting conic sections to scattered data. *Computer Graphics and Image Processing* 9, 56–71 (1979)
2. Csetverikov, D.: Basic algorithms for digital image analysis, Course, Institute of Informatics, Eotvos Lorand University, visual.ipan.sztaki.hu

3. Davies, E.R.: Algorithms for ultra-fast location of ellipses in digital images. *Proc. IEE Image Processing and its Applications* 2, 542–546 (1999)
4. Fitzgibbon, A.W., Pilu, M., Fisher, R.B.: Direct least square fitting of ellipses. *IEEE T-PAMI* 21(5), 476–480 (1999)
5. Koprnicky, M., Ahmed, M., Kamel, M.: Contour description through set operations on dynamic reference shapes. In: Campilho, A., Kamel, M. (eds.) *ICIAR 2004*. LNCS, vol. 3211, pp. 400–407. Springer, Heidelberg (2004)
6. Proffitt, D.: The Measurement of Circularity and Ellipticity on a Digital Grid. *Pattern Recognition* 15(5), 383–387 (1982)
7. Peura, M., Iivarinen, J.: Efficiency of simple shape descriptors. In: Arcelli, C., Cordella, L.P., Sanniti di Baja, G. (eds.) *Advances in Visual Form Analysis*, World Sci. (1997)
8. Rosin, P.L.: Ellipse fitting using orthogonal hyperbolae and Stirling's oval. *CVGIP: Graph Models Image Process* 60(3), 209–213 (1998)
9. Rosin, P.L.: Further five-point fit ellipse fitting. *CVGIP: Graph Models Image Proc.* 61(5), 245–259 (1999)
10. Rosin, P.L.: Measuring shape: ellipticity, rectangularity, and triangularity. *Machine Vision and Applications* 14, 172–184 (2003)
11. Rosin, P.L.: Assessing error of fit functions for ellipses. *CVGIP: Graph Models Image Process* 58(5), 494–502 (1996)
12. Rothe, I., Süße, H., Voss, K.: The method of normalization to determine invariants. *IEEE T-PAMI* 18(4), 366–376 (1996)
13. Rosin, P.L., Zunic, J.: 2D shape measures for computer vision. In: *Handbook of Applied Algorithms: Solving Scientific, Engineering and Practical problems*, Wiley, Chichester (2007)
14. Stojmenovic, M., Nayak, A., Zunic, J.: Measuring Linearity of a Finite Set of Points. In: *IEEE International Conference on Cybernetics and Intelligent Systems (CIS)*, Bangkok, Thailand, pp. 222–227 (2006)
15. Tuset, V.M., Rosin, P.L., Lombarte, A.: Sagittal otolith shape used in the identification of fishes of the genus *Serranus*. *Fisheries Research* 81, 316–325 (2006)
16. Voss, K., Süße, H.: Invariant fitting of planar objects by primitives. *IEEE T-PAMI* 19, 80–84 (1997)
17. Zhang, S.C., Liu, Z.Q.: A robust, real time ellipse detector. *Pattern Recognition* 38, 273–287 (2005)